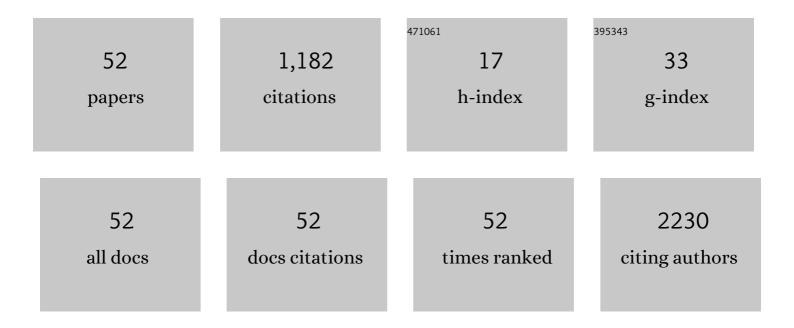
Tae Sup Lee

List of Publications by Year in descending order

Source: https://exaly.com/author-pdf/6351272/publications.pdf Version: 2024-02-01



TAE SUD LEE

#	Article	IF	CITATIONS
1	Therapeutic Response Monitoring with 89Zr-DFO-Pertuzumab in HER2-Positive and Trastuzumab-Resistant Breast Cancer Models. Pharmaceutics, 2022, 14, 1338.	2.0	3
2	CXCR4 uses STAT3-mediated slug expression to maintain radioresistance of non-small cell lung cancer cells: emerges as a potential prognostic biomarker for lung cancer. Cell Death and Disease, 2021, 12, 48.	2.7	16
3	An antibody against L1 cell adhesion molecule inhibits cardiotoxicity by regulating persistent DNA damage. Nature Communications, 2021, 12, 3279.	5.8	12
4	Development of ⁶⁴ Cu-NOTA-Trastuzumab for HER2 Targeting: A Radiopharmaceutical with Improved Pharmacokinetics for Human Studies. Journal of Nuclear Medicine, 2019, 60, 26-33.	2.8	47
5	PET imaging of HER2 expression with an 18F-fluoride labeled aptamer. PLoS ONE, 2019, 14, e0211047.	1.1	32
6	Development of a Theranostic Convergence Bioradiopharmaceutical for Immuno-PET Based Radioimmunotherapy of L1CAM in Cholangiocarcinoma Model. Clinical Cancer Research, 2019, 25, 6148-6159.	3.2	14
7	Facile metabolic glycan labeling strategy for exosome tracking. Biochimica Et Biophysica Acta - General Subjects, 2018, 1862, 1091-1100.	1.1	62
8	A cell surface clicked navigation system to direct specific bone targeting. Bioorganic and Medicinal Chemistry, 2018, 26, 758-764.	1.4	2
9	Anti-EGFR lipid micellar nanoparticles co-encapsulating quantum dots and paclitaxel for tumor-targeted theranosis. Nanoscale, 2018, 10, 19338-19350.	2.8	45
10	PET Imaging Biomarkers of Anti-EGFR Immunotherapy in Esophageal Squamous Cell Carcinoma Models. Cells, 2018, 7, 187.	1.8	5
11	Monitoring of macrophage accumulation in statin-treated atherosclerotic mouse model using sodium iodide symporter imaging system. Nuclear Medicine and Biology, 2017, 48, 45-51.	0.3	2
12	A Bioluminogenic Probe for Monitoring Tyrosinase Activity. Chemistry - an Asian Journal, 2017, 12, 397-400.	1.7	13
13	Cancer-targeted Nucleic Acid Delivery and Quantum Dot Imaging Using EGF Receptor Aptamer-conjugated Lipid Nanoparticles. Scientific Reports, 2017, 7, 9474.	1.6	54
14	Combination of anti-L1 cell adhesion molecule antibody and gemcitabine or cisplatin improves the therapeutic response of intrahepatic cholangiocarcinoma. PLoS ONE, 2017, 12, e0170078.	1.1	10
15	Immuno-PET imaging based radioimmunotherapy in head and neck squamous cell carcinoma model. Oncotarget, 2017, 8, 92090-92105.	0.8	20
16	lmmuno-PET Imaging and Radioimmunotherapy of ⁶⁴ Cu-/ ¹⁷⁷ Lu-Labeled Anti-EGFR Antibody in Esophageal Squamous Cell Carcinoma Model. Journal of Nuclear Medicine, 2016, 57, 1105-1111.	2.8	54
17	In vivo monitoring of CD44+ cancer stem-like cells by γ-irradiation in breast cancer. International Journal of Oncology, 2016, 48, 2277-2286.	1.4	15
18	Evaluation of safety and efficacy of adipose-derived stem cells in rat myocardial infarction model using hexadecyl-4-[124 I]iodobenzoate for cell tracking. Applied Radiation and Isotopes, 2016, 108, 116-123.	0.7	2

TAE SUP LEE

#	Article	IF	CITATIONS
19	Hybridization-based aptamer labeling using complementary oligonucleotide platform for PET and optical imaging. Biomaterials, 2016, 100, 143-151.	5.7	23
20	Detection of metastatic tumors after γ-irradiation using longitudinal molecular imaging and gene expression profiling of metastatic tumor nodules. International Journal of Oncology, 2016, 48, 1361-1368.	1.4	1
21	Evaluation of diethylnitrosamine- or hepatitis B virus X gene-induced hepatocellular carcinoma with 18F-FDG PET/CT: A preclinical study. Oncology Reports, 2015, 33, 347-353.	1.2	6
22	Assessment of α-Fetoprotein Targeted HSV1- <i>tk</i> Expression in Hepatocellular Carcinoma with <i>In Vivo</i> Imaging. Cancer Biotherapy and Radiopharmaceuticals, 2015, 30, 8-15.	0.7	12
23	Generation of a human antibody that inhibits TSPAN8-mediated invasion of metastatic colorectal cancer cells. Biochemical and Biophysical Research Communications, 2015, 468, 774-780.	1.0	20
24	Evaluation of a 64Cu-labeled 1,4,7-triazacyclononane, 1-glutaric acid-4,7 acetic acid (NODAGA)-galactose-bombesin analogue as a PET imaging probe in a gastrin-releasing peptide receptor-expressing prostate cancer xenograft model. International Journal of Oncology, 2015, 46, 1159-1168.	1.4	7
25	Simple Methods for Tracking Stem Cells with ⁶⁴ Cu-Labeled DOTA-hexadecyl-benzoate. ACS Medicinal Chemistry Letters, 2015, 6, 528-530.	1.3	14
26	Longitudinal monitoring adipose-derived stem cell survival by PET imaging hexadecyl-4-124l-iodobenzoate in rat myocardial infarction model. Biochemical and Biophysical Research Communications, 2015, 456, 13-19.	1.0	17
27	Extension of the in vivo half-life of endostatin and its improved anti-tumor activities upon fusion to a humanized antibody against tumor-associated glycoprotein 72 in a mouse model of human colorectal carcinoma. Oncotarget, 2015, 6, 7182-7194.	0.8	12
28	Detection of Increased ⁶⁴ Cu Uptake by Human Copper Transporter 1 Gene Overexpression Using PET with ⁶⁴ CuCl ₂ in Human Breast Cancer Xenograft Model. Journal of Nuclear Medicine, 2014, 55, 1692-1698.	2.8	44
29	Cetuximab inhibits cisplatin-induced activation of EGFR signaling in esophageal squamous cell carcinoma. Oncology Reports, 2014, 32, 1188-1192.	1.2	11
30	RGD Peptide–Conjugated Multimodal NaGdF ₄ :Yb ³⁺ /Er ³⁺ Nanophosphors for Upconversion Luminescence, MR, and PET Imaging of Tumor Angiogenesis. Journal of Nuclear Medicine, 2013, 54, 96-103.	2.8	125
31	In Vitro Radionuclide Therapy and In Vivo Scintigraphic Imaging of Alpha-Fetoprotein-Producing Hepatocellular Carcinoma by Targeted Sodium Iodide Symporter Gene Expression. Nuclear Medicine and Molecular Imaging, 2013, 47, 1-8.	0.6	15
32	Synthesis and Evaluation of a ¹⁸ F-Labeled 4-Ipomeanol as an Imaging Agent for CYP4B1 Gene Prodrug Activation Therapy. Cancer Biotherapy and Radiopharmaceuticals, 2013, 28, 588-597.	0.7	4
33	In vitro monitoring of cardiomyogenic differentiation of mesenchymal stem cells using sodium iodide symporter gene. Tissue Engineering and Regenerative Medicine, 2012, 9, 304-310.	1.6	3
34	Imaging of a localized bacterial infection with endogenous thymidine kinase using radioisotope-labeled nucleosides. International Journal of Medical Microbiology, 2012, 302, 101-107.	1.5	14
35	<i>In vivo</i> bioluminescent imaging of αâ€fetoproteinâ€producing hepatocellular carcinoma in the diethylnitrosamineâ€treated mouse using recombinant adenoviral vector. Journal of Gene Medicine, 2012, 14, 513-520.	1.4	12
36	Persistent infection of a gammaherpesvirus in the central nervous system. Virology, 2012, 423, 23-29.	1.1	9

TAE SUP LEE

#	Article	IF	CITATIONS
37	Gamma camera and optical imaging with a fusion reporter gene using human sodium/iodide symporter and monomeric red fluorescent protein in mouse model. International Journal of Radiation Biology, 2011, 87, 1182-1188.	1.0	2
38	Amphiphilic polymer-coated hybrid nanoparticles as CT/MRI dual contrast agents. Nanotechnology, 2011, 22, 155101.	1.3	124
39	Non-invasive monitoring of hepatocellular carcinoma in transgenic mouse with bioluminescent imaging. Cancer Letters, 2011, 310, 53-60.	3.2	11
40	Modulation of Insulin Sensitivity and Caveolin-1 Expression by Orchidectomy in a Nonobese Type 2 Diabetes Animal Model. Molecular Medicine, 2011, 17, 4-11.	1.9	18
41	Radioiodination and biodistribution of quantum dots using Bolton–Hunter reagent. Applied Radiation and Isotopes, 2011, 69, 56-62.	0.7	7
42	Association Between Age at Diagnosis and the Presence of EGFR Mutations in Female Patients with Resected Non-small Cell Lung Cancer. Journal of Thoracic Oncology, 2010, 5, 1949-1952.	0.5	36
43	Prodrug-activating Gene Therapy with Rabbit Cytochrome P450 4B1/4-Ipomeanol or 2-Aminoanthracene System in Glioma Cells. Nuclear Medicine and Molecular Imaging, 2010, 44, 193-198.	0.6	8
44	Characterization and Cancer Cell Specific Binding Properties of Anti-EGFR Antibody Conjugated Quantum Dots. Bioconjugate Chemistry, 2010, 21, 940-946.	1.8	65
45	Application of bioluminescence imaging to therapeutic intervention of herpes simplex virus type I – Thymidine kinase/ganciclovir in glioma. Cancer Letters, 2010, 297, 84-90.	3.2	12
46	Comparison of 18F-FDG, 18F-FET and 18F-FLT for differentiation between tumor and inflammation in rats. Nuclear Medicine and Biology, 2009, 36, 681-686.	0.3	78
47	Registration Method for the Detection of Tumors in Lung and Liver Using Multimodal Small Animal Imaging. IEEE Transactions on Nuclear Science, 2009, 56, 1454-1458.	1.2	5
48	Anesthesia condition for 18F-FDG imaging of lung metastasis tumors using small animal PET. Nuclear Medicine and Biology, 2008, 35, 143-150.	0.3	38
49	Experimental condition and registration method for the tumor detection of lung metastasis small animal PET and CT whole body images. , 2007, , .		2
50	<i>Short Commmunication:</i> Synthesis and Biologic Evaluation of I-123-Labeled Porphyrin Derivative as a Potential Tumor-Imaging Agent. Cancer Biotherapy and Radiopharmaceuticals, 2007, 22, 853-862.	0.7	7
51	Syntheses of F-18 labeled fluoroalkyltyrosine derivatives and their biological evaluation in rat bearing 9L tumor. Bioorganic and Medicinal Chemistry Letters, 2007, 17, 200-204.	1.0	12
52	Respiratory Gating of MicroPET and Clinical CT Studies Using List-mode Acquisition. , 2006, , .		0